Article citation info:
Szymański GM, Cywka B, Mokrzan D, Prokopowicz W. Estimation of fuel consumption in a jet engine based on vibration signal parameters. Combustion Engines. 2023;194(3):13-20. https://doi.org/10.19206/CE-166278

Grzegorz Marek SZYMAŃSKI
Bartłomiej CYWKA
Daniel MOKRZAN
Wojciech PROKOPOWICZ

Combustion Engines
Polish Scientific Society of Combustion Engines

Estimation of fuel consumption in a jet engine based on vibration signal parameters

ARTICLE INFO

Received: 15 March 2023
Revised: 17 April 2023
Accepted: 17 May 2023
Available online: 1 June 2023

This paper proposes the use of vibroacoustic signal parameters to estimate the fuel consumption of a miniature GTM-400 engine. The method for testing engine vibrations is presented, followed by an analysis of the results obtained. Two vibration point measures were selected to build a fuel consumption model. The models obtained were verified, after which those that best describe the real fuel consumption of the engine were selected. The paper proves that the vibration signal, in addition to its applications in jet engine diagnostics, can be used to determine engine performance, which can contribute to reducing the complexity of construction and increasing the economics of engine operation.

Key words: *vibroacoustics, jet engine, fuel consumption, estimation, statistical analysis*

1. Introduction

Today, one of the requirements of machines is to achieve the highest possible levels of efficiency. For machines with rotating components, this problem is often optimised by increasing their rotational speed [22]. Due to the impossibility of perfectly balanced rotors, some energy is converted into oscillations [1, 14, 19]. Unwanted oscillations can cause damage or failure, so it is important to monitor them properly at all times. The analysis of vibration measurements of equipment, characterised not only by the high precision in determining the damaged components and the type of damage [7, 26, 31], but also by the possibility of continuously monitoring their condition [21]. In addition, the analysis of the vibroacoustic signal can be used to determine the operating parameters of the machinery. In the papers [4, 24, 32] the authors proposed using the time-frequency representation of the vibration signal to determine the instantaneous shaft speed of the wind turbine gearbox and the internal combustion engine. The authors of the study presented in [13] showed that the use of a vibroacoustic signal and wavelet transformation can be used to identify the composition of the fuel used to power the engine. However, in this article, the authors have proposed the use of vibration signal parameters to estimate the fuel consumption of a GTM-400 miniature turbine jet engine.

Currently, many methods have been developed to measure the mass flow rate of fluids. Referring to the work [28] flow meters can be divided into four groups, depending on the parameter directly measured by them, i.e.: velocity, volume, mass, indirect parameters (e.g. differential pressure).

Most for the methods of measuring fluid output affect the pressure drop of the flowing fluid [11]. In addition, each of these methods requires the installation of dedicated sensor in a strictly defined location on the equipment, which increases the complexity of the design, production costs, and machine operation [5, 18]. The method proposed in this paper allows the use of a vibroacoustic signal, nowadays increasingly used for diagnostic purposes [3], to estimate the mass intensity of the fuel that feeds a turbine engine. The advantages of using this method to determine fuel flow rate are the high accuracy of the estimation, the lack of interference with the fluid flow, and the increased economy of the design.

2. Vibration test methods for aircraft engines

Nowadays for most aircraft engines in service by condition, it is essential to collect data on the vibration of its components [10, 20]. In paper [29], the author proposed a classification of vibration transducers according to the measured parameter (displacement, velocity, acceleration), the need for power supply (active and passive transducers), the relative or absolute measurement of vibrations and the contact or lack thereof with the object under test. Each transducer has its limitations, related to its operating principle. Turbine engines, due to their high rotor speeds, are characterised by high-frequency vibrations, and therefore the most accurate measurements of their vibrations are obtained using accelerometers. The most commonly used acceleration sensor is a piezoelectric crystal. These sensors produce an electrical signal in response to dynamic loads; however, due to the high impedance of the system, piezoelectric sensors require converters to transform the signal into one suitable for the rest of the system [1, 2].

With device-mounted vibration transducers, the strongest signal and one with the least interference can be obtained at or as close to the rotating component as possible. For design reasons, this is often not feasible. The solution that gives the best results, as presented in the [19, 30] works, is to test vibrations in the motor bodies, in the immediate vicinity of the bearings.

All machine-mounted transducers have their own mass; for vibration measurements of lightweight structures, the mass of the sensors can affect the results obtained. Some machines, due to their design, do not allow the use of vibration transducers mounted on their structure. In these cases, the use of noncontact vibration sensors is justified. Most noncontact vibration sensors operate on the principle of emitting and receiving laser light reflected from the structure [33].

The use of a vibroacoustic signal in the machine diagnosis process enables the detection of malfunctions before they lead to damage and allows the indication of faulty components. This reduces operating costs by reducing the frequency of servicing, replacement of individual engine units, and faster removal of malfunctions. In addition, continuous inspection of the aircraft structure results in increased flight safety and, through more efficient use of engine components, reduces the negative impact on the environment [6, 16].

3. Research methodology

The subject of the study was a GTM-400 miniature turbine jet engine with a thrust of 400 N, built on a test stand. The engine has a single-rotor design. There is a single 14-blade radial compressor stage on the shaft and a single-stage 23-blade axial turbine. The engine has an annular combustion chamber with backflow and an uncontrollable convergent nozzle. The rotor is supported by two ball bearings. An electric starting system, fuel pump, engine control module, and battery are built into the engine. The maximum engine speed is 80,000 rpm. The following sensors were placed on the test stand: temperature and pressure of the working medium, engine thrust and mass intensities of fuel and air. The engine diagram is shown in Fig. 1.

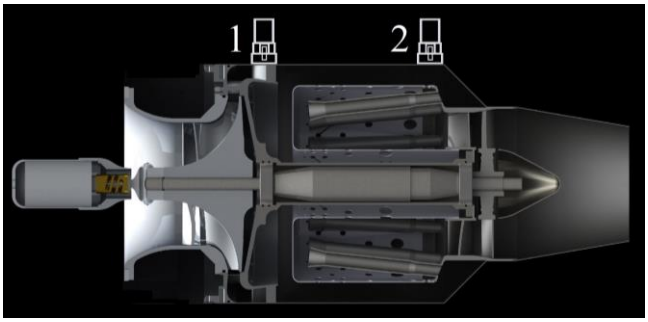

Fig. 1. Diagram of the GTM-400 motor with schematic representation of the accelerators 1, 2

To test the vibration parameters of the motor, three 'TYPE 4391' piezo transducers from Brüel & Kjær were attached to the body and test stand. CCLD transducers 'TYPE 2647' also from Brüel & Kjær were used for impedance matching of the sensors. Picture of the engine with the transducers attached to it is shown in Fig. 2.

The use of uniaxial transducers was necessary due to the high temperatures reached by the surfaces to which the sensors were attached [25]. Accelerometers were screwed onto pads previously glued to the test object. Cyanoacrylate adhesive was used. The method used to attach the transducers allows for correct measurements to be obtained and does not require interference with the engine structure. The disadvantages of the method used include the need for a prior preparation of the surface to be bonded and temperature limitations related to the properties of the glue [27]. Transducers process the vibration signal in the axis perpendicular to test stand. Transducer 1 was mounted in the fan bearing plane. In order to measure vibrations in the same axis as transducer 1, transducer 2 was not mounted in the plane of the turbine bearing, but as close as possible to the turbine. Transducer 1 is significantly larger than the other because the adapter that was previously mounted to it has been left on. The adapter does not affect the operation of the transducer, it was not removed for service reasons – to avoid wear on the accelerometer threads. The test bench shown in Fig. 2 is not a proposal for a fully developed system and is only used to investigate the possibility of using vibroacoustic parameters to estimate fuel consumption.

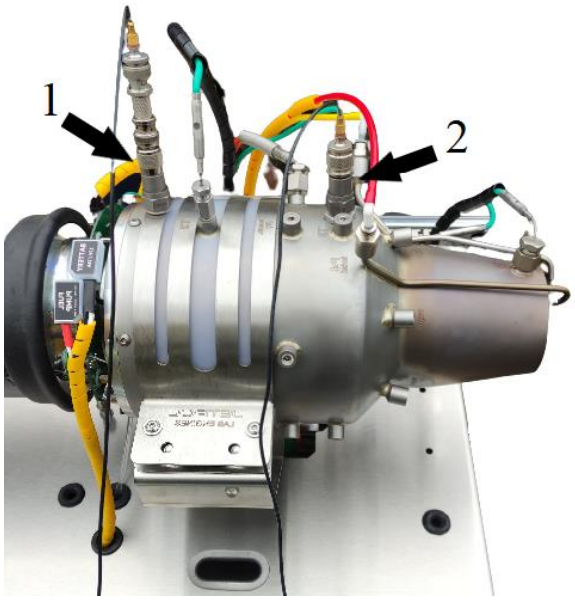

Fig. 2. Location of accelerometers on the test bench

4. Analysis of research results

4.1. Results of fuel consumption measurements

Research into the estimation of the fuel consumption of a jet engine required measuring the amount of fuel delivered to the combustion chamber. The engine control system was used to measure this amount. Measurements were made at a sampling rate of 10 Hz and performed for seven operating settings of the engine. The results in Table 1 are the averages of 100 measurements.

Table 1. Results of jet engine fuel consumption measurements

Setup of engine power	Fuel consumption [ml/min]	Deviation of fuel consumption [ml/min]
1	240.26	3.48
2	378.08	3.29
3	469.87	5.75
4	587.86	6.12
5	769.99	5.31
6	1043.17	5.20
7	1135.20	10.12

4.2. Analysis of vibration measurement results

One method of describing vibration signals in the amplitude domain is the use of point measures [9, 12, 19]. They allow the vibration signal to be characterised by a single number. Thanks to this description of the vibration parameters, it is easy to determine changes in the vibroacoustic signal resulting from changes in the state of the object. Point measures used in vibroacoustic diagnostics can be

divided according to the work [8] into dimensions and dimensionless. The dimensional point measures most commonly used for analysis include [9, 17]:

– effective amplitude:

$$s_{RMS} = \sqrt{\frac{1}{N}\sum_{i=1}^{N}(s_i)^2} \tag{1}$$

where: s_i is instantaneous signal value, N is number of signal samples analysed.

Takes greater account of large values of instantaneous amplitude, is sensitive to the occurrence of high amplitudes and is the most commonly used point measure due to its proportionality to process power. In view of the previous points, and the fact that high power processes occur at the test points, for the purposes of this study, RMS describes the processes taking place better than average amplitude,

– peak amplitude:

$$s_{PEAK} = \max|(s_i)| \tag{2}$$

is used to evaluate impulse processes, e.g. clearance, impact, etc.

Dimensionless discriminants are quotients of the corresponding dimensional score measures, they include, but are not limited to, the following:

– crest factor:

$$CF = \frac{s_{PEAK}}{s_{RMS}} \tag{3}$$

– kurtosis:

$$\beta = \frac{\frac{1}{N}\sum_{i=1}^{N}(s_i)^4}{\left[\frac{1}{N}\sum_{i=1}^{N}(s_i)^2\right]^2} \tag{4}$$

Figure 3 shows the time course of the vibration acceleration signals recorded during the jet engine tests.

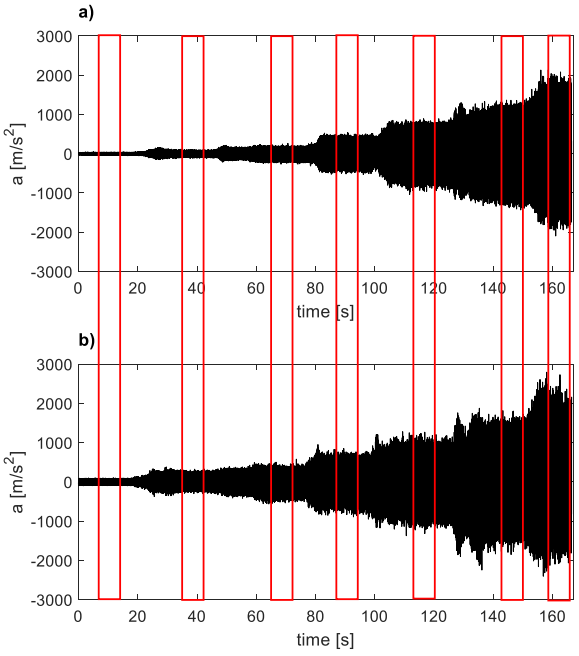

Fig. 3. Time history of vibration signals: a) recorded on the fan bearing axis, b) recorded on the turbine bearing axis

The red rectangles indicate the time windows in which the signal was analysed for different motor operating settings. The results of the point measure calculations for the vibration accelerations recorded in the fan bearing axis are shown in Table 2.

Table 2. Measurement results of vibration acceleration parameters recorded in the fan bearing axis

Setup of engine power	Crest Factor [–]	Kurtosis [–]	a_{PEAK} [m/s]^2	a_{RMS} [m/s]^2
1	5.48	3.09	54.33	9.92
2	4.98	2.96	114.04	25.39
3	4.43	2.84	264.05	60.09
4	2.99	1.93	538.30	179.80
5	3.85	2.44	892.45	269.36
6	3.10	2.05	1365.59	462.34
7	2.46	1.72	2082.55	851.68

Figure 4 shows the variation of the vibration acceleration parameters (recorded on the fan bearing axis) as a function of the engine fuel consumption at different operating points.

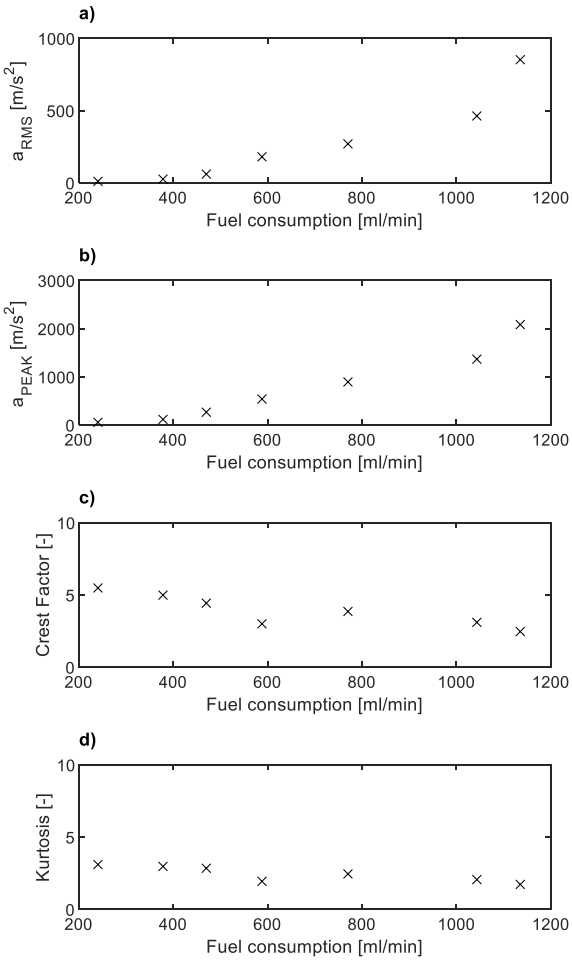

Fig. 4. Dependence of point measures of vibration signals a) RMS, b) PEAK, c) Crest Factor, d) Kurtosis, recorded in the fan bearing axis on fuel consumption

The results of the point measure calculations for the vibration accelerations recorded on the turbine bearing axis are shown in Table 3.

Table 3. Results of measurements of vibration acceleration parameters recorded on the turbine bearing axis

Setup of engine power	Crest Factor [–]	Kurtosis [–]	a_{PEAK} $[m/s]^2$	a_{RMS} $[m/s]^2$
1	5.62	3.31	139.58	24.89
2	4.47	2.87	333.85	74.71
3	4.73	2.94	579.82	122.53
4	4.66	2.88	852.26	203.27
5	4.38	2.68	1280.56	312.64
6	4.07	2.71	1816.91	454.68
7	4.42	2.93	2730.94	617.68

Changes in vibration acceleration parameters (recorded on the turbine bearing axis) in relation to the fuel consumption of the engine at different operating points are shown in Fig. 5.

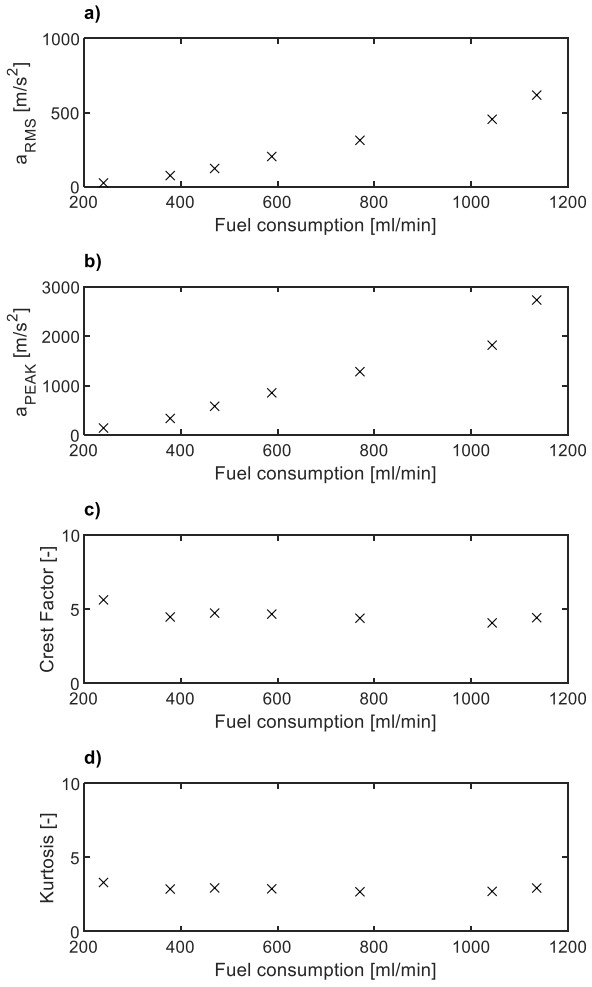

Fig. 5. Dependence of point measures of vibration signals a) RMS, b) PEAK, c) Crest Factor, d) Kurtosis, recorded at the turbine bearing axis on fuel consumption

Based on an analysis of Fig. 4 and 5, it was concluded that, for further research, a_{RMS} and $_{aPEAK}$ measures will be used, as the values of the kurtosis and crest factor do not meet the conditions of the explanatory variable in the modelling process (unambiguity and sufficient width of the field of change relative to the explanatory variable).

4.3. Fuel consumption modelling

One method to find the relationship between dependent and independent variables is to develop a model using statistical analysis tools. Least squares regression analysis is most commonly used to develop models, which in the general case can be written with the equation [23]:

$$\mathbf{Y} = \mathbf{X} \cdot \beta + \varepsilon \tag{5}$$

where: $\mathbf{Y}$ – vector of explanatory variable, β – vector of model coefficients, $\mathbf{X}$ – matrix of the explanatory variables, ε is the i-th noise term, that is, random error.

The study proposed five models described by equations (6–10). The models were named as follows: power1 – equation (6), power2 – equation (7), polly1 – equation (8), polly2 – equation (9), exp1 – equation (10).

$$FC^{power1}(a) = \beta_1 \cdot a^{\beta_2} \tag{6}$$

$$FC^{power2}(a) = \beta_1 \cdot a^{\beta_2} + \beta_3 \tag{7}$$

$$FC^{poly1}(a) = \beta_1 \cdot a + \beta_2 \tag{8}$$

$$FC^{poly2}(a) = \beta_1 \cdot a^2 + \beta_2 \cdot a + \beta_3 \tag{9}$$

$$FC^{exp}(a) = \beta_1 \cdot \exp(\beta_2 \cdot a) \tag{10}$$

where: FC is fuel consumption, a is parameter of vibration acceleration, β_i are model coefficient.

The results of modelling using the RMS value of vibration accelerations recorded at the fan bearing axis are shown in Fig. 6, while a graphical interpretation of the modelling results, in which the explanatory variable was the peak value of vibration accelerations, is shown in Fig. 7.

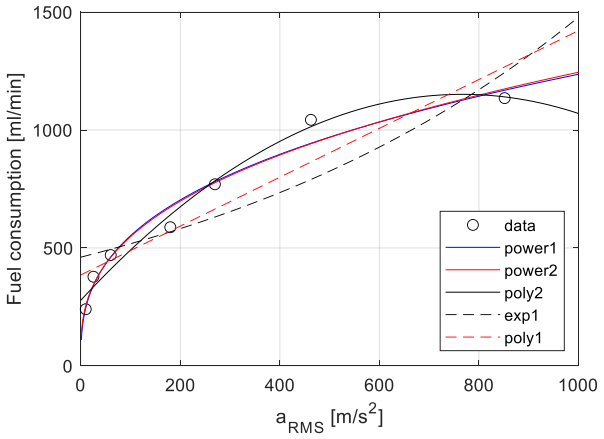

Fig. 6. Relationship between the fuel consumption of the tested jet engine and the RMS value of the vibration acceleration recorded on the fan bearing axis

Figure 8 shows the results of the modelling using an explanatory variable in the form of the RMS value of the vibration accelerations recorded on the turbine bearing axis, and Fig. 9 shows a graphical interpretation of the modelling results using the peak value of the vibration accelerations.

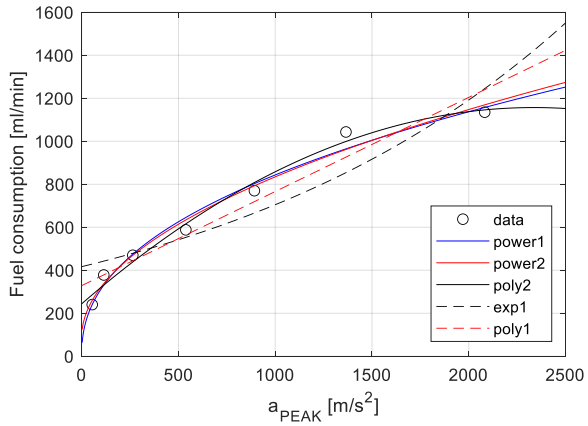

Fig. 7. Relationship between the fuel consumption of the tested jet engine and the maximum value of vibration accelerations recorded on the fan bearing axis

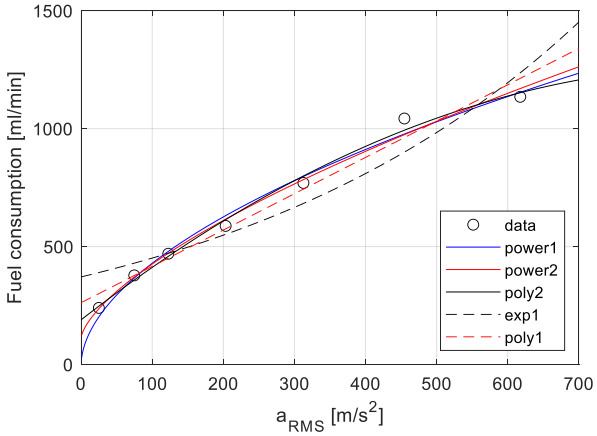

Fig. 8. Relationship between the fuel consumption of the tested jet engine and the RMS value of the vibration acceleration recorded on the turbine bearing axis

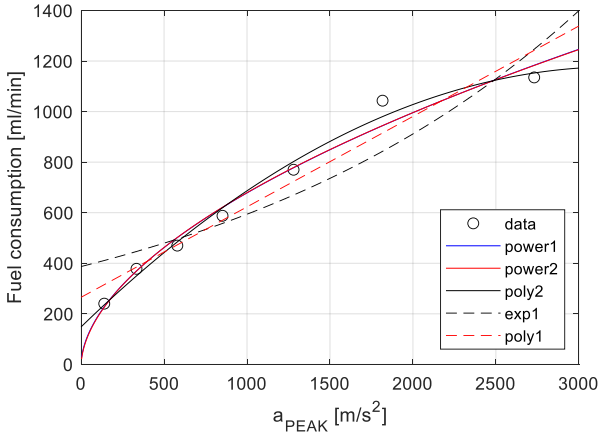

Fig. 9. Relationship between the fuel consumption of the tested jet engine and the maximum value of vibration accelerations recorded on the turbine bearing axis

Based on the analysis of Fig. 6–9, it was found that the model described by the exponential function (10), cannot be used to model the fuel consumption of a jet engine from vibration signals, as its course is divergent from the trend of the analysed data. Therefore, the model verification process was limited to the power and polynomial functions described by equations (6–9).

4.4. Verification of the models

Regression models determined by the least squares method should be statistically verified. The verification of the determined models was caried out by determining a series of statistics. First, the degree of fit of the model to the real data was determined. For this purpose, the coefficient of determination R^2 was determined, which indicates how much of the variability in the explained variable was explained by the model. As part of the model verification, statistical tests were performed to verify the significance of the regression model coefficients using Snedecor's F distribution. On the other hand, the Student's t distribution was used to test hypotheses to determine the significance of individual regression coefficients [15]. During the regression model verification process, a significance level of 0.05 was assumed. It was determined that a regression model would be positively verified if: the coefficient of determination is greater than or equal to 0.80, the model coefficients are statistically significant (F-value and pValue < 0.05).

Tables 4 and 5 show the results of the verification of the model in which the explanatory variable was the RMS value of the vibration accelerations recorded on the bearing axis of the fan.

Table 4. Results of verification of power models based on the RMS value of vibration accelerations recorded on the fan bearing axis

Estimated coefficients	$a_{RMS-FUN}$			
	power1		power2	
	$R^2 = 0.97$		$R^2 = 0.97$	
	F= 2.28e–06		F = 0.0009	
	Estimate	pValue	Estimate	pValue
β_1	110.1	0.0042	88.6	0.44
β_2	0.35	0.00014	0.38	0.066
β_3	–	–	44.3	0.85

Table 5. Results of verification of polynomial models based on the RMS value of vibration accelerations recorded in the fan bearing axis

Estimated coefficients	$a_{RMS-FUN}$			
	poly1		poly2	
	$R^2 = 0.87$		$R^2 = 0.98$	
	F = 0.002		F = 0.0003	
	Estimate	pValue	Estimate	pValue
β_1	1.04	0.002	–0.0014	0.0087
β_2	385.7	0.0024	2.28	0.001
β_3	–	–	278.4	0.0016

Based on the analysis of the results in Tables 4 and 5 and Fig. 6, it was concluded that the power2 model should be discarded because its coefficients are not statistically significant and the poly2 model because there is a local extreme in the model, which results in the model not meeting the unambiguity condition.

Tables 6 and 7 show the results of the model verification based on the maximum value of the vibration accelerations recorded on the axis of the fan bearing.

Analysis of the results in Tables 5 and 6 and Fig. 7 made it possible to conclude that the power2 and polly2

models could not be used for modelling for the same reasons as for models based on the RMS value of vibration accelerations.

Table 6. Results of the verification of power models based on the maximum value of vibration accelerations recorded on the fan bearing axis

Estimated coefficients	$a_{PEAK-FUN}$			
	power1		power2	
	$R^2 = 0.98$		$R^2 = 0.98$	
	F = 7.64e–07		F = 0.00033	
	Estimate	pValue	Estimate	pValue
β_1	42.9	0.0081	22.65	0.46
β_2	0.43	5.09e–05	0.51	0.026
β_3	–	–	88.9	0.57

Table 7. Polynomial model verification results based on the maximum value of vibration accelerations recorded on the axis of the fan bearing

Estimated coefficients	$a_{PEAK-FUN}$			
	poly1		poly2	
	$R^2 = 0.94$		$R^2 = 0.99$	
	F = 0.00031		F = 0.00019	
	Estimate	pValue	Estimate	pValue
β_1	0.43	0.0003	–0.00016	0.022
β_2	328.5	0.0013	7.92	0.0013
β_3	–	–	6.76	0.0024

Tables 8 and 9 show the results of the verification of the models based on the peak value of the vibration accelerations recorded on the turbine bearing axis.

Table 8. Results of verification of power models based on the RMS value of vibration accelerations recorded on the turbine bearing axis

Estimated coefficients	$a_{RMS-TURBINE}$			
	power1		power2	
	$R^2 = 0.99$		$R^2 = 0.99$	
	F = 2.88e–07		F = 0.0001	
	Estimate	pValue	Estimate	pValue
β_1	35.3	0.0048	14.5	0.32
β_2	0.54	2.03e–05	0.66	0.0063
β_3	–	–	112.5	0.28

Table 9. Results of verification of polynomial models based on the RMS value of vibration accelerations recorded at the turbine bearing axis

Estimated coefficients	$a_{RMS-TURBINE}$			
	poly1		poly2	
	$R^2 = 0.97$		$R^2 = 0.99$	
	F = 3.61e–05		F = 5.21e–05	
	Estimate	pValue	Estimate	pValue
β_1	1.54	3.61e-05	–0.0012	0.053
β_2	262.5	0.0008	2.35	0.0008
β_3	–	–	189.8	0.0037

Based on the analysis of the results in Tables 8 and 9, it was concluded that the power2 and poly2 models should be discarded as their coefficients are not statistically significant.

Tables 10 and 11 show the results of the model verification based on the maximum value of the vibration accelerations recorded on the turbine bearing axis.

Table 10. Results of the verification of power models based on the maximum value of vibration accelerations recorded at the turbine bearing axis

Estimated coefficients	$a_{PEAK-TURBINE}$			
	power1		power2	
	$R^2 = 0.98$		$R^2 = 0.98$	
	F = 9.36e–07		F = 0.000451	
	Estimate	pValue	Estimate	pValue
β_1	14.8	0.027	15.62	0.55
β_2	0.55	5.61e–05	0.54	0.037
β_3	–	–	–7.26	0.97

Table 11. Polynomial model verification results based on the maximum value of vibration accelerations recorded on the turbine bearing axis

Estimated coefficients	$a_{PEAK-TURBINE}$			
	poly1		poly2	
	$R^2 = 0.95$		$R^2 = 0.98$	
	F = 0.0002		F = 0.00011	
	Estimate	pValue	Estimate	pValue
β_1	0.36	0.0002	–9.85e–05	0.056
β_2	265.5	0.0039	0.63	0.0009
β_3	–	–	148.3	0.0201

The analysis of the results in Tables 10 and 11 allowed us to conclude that the power2 and polly2 models could not be used for modelling, as their coefficients are not statistically significant.

On the basis of the verification carried out, the following models were found to meet the criteria for the signals recorded on the fan bearing axis:

$$FC^{power1}_{a_{RMS-FUN}}(a) = 110.1\, a^{0.35}_{RMS-FUN} \quad (11)$$

$$FC^{polly1}_{a_{RMS-FUN}}(a) = 1.04\, a_{RMS-FUN} + 385.7 \quad (12)$$

$$FC^{power1}_{a_{PEAK-FUN}}(a) = 42.9\, a^{0.43}_{PEAK-FUN} \quad (13)$$

$$FC^{polly1}_{a_{PEAK-FUN}}(a) = 0.43\, a_{PEAK-FUN} + 328.5 \quad (14)$$

However, for signals recorded on the turbine bearing axis, the models described by the equations can be used:

$$FC^{power1}_{a_{RMS-TURBINE}}(a) = 35.3\, a^{0.54}_{RMS-TURBINE} \quad (15)$$

$$FC^{polly1}_{a_{RMS-TURBINE}}(a) = 1.54\, a_{RMS\,-\,TURBINE} + 262.5 \quad (16)$$

$$FC^{power1}_{a_{PEAK-TURBINE}}(a) = 14.8\, a^{0.55}_{PEAK-TURBINE} \quad (17)$$

$$FC^{polly1}_{a_{PEAK-TURBINE}}(a) = 0.36 \cdot a_{PEAK-TURBINE} + 265.5 \quad (18)$$

Based on an analysis of the fit of the models to the input data based on R^2, it was concluded that for the vibration acceleration parameters recorded in the fan bearing axis, the

model described by Eq. (13) is the best used and for the data recorded in the turbine bearing axis by relation (15).

5. Conclusions

This paper presents a method to measure the vibrations of the GTM-400 miniature turbine engine and proposes models of its fuel consumption using point measurements of the vibroacoustic signal. A verification of the proposed models was carried out, and it was determined which models describe fuel consumption the most accurately. Based on the research carried out, it can be shown that:

- vibroacoustic signal parameters can be used to analyse many aspects of machine operation,
- measures of effective and peak amplitude allow the fuel consumption model of the GTM-400 engine to be created,
- kurtosis and crest factor do not fulfil the conditions of an explanatory variable in the modelling of the fuel consumption of the engine under investigation,
- the use of an exponential function does not allow a correct fuel consumption model to be proposed,
- the proposed fuel consumption models provide a high level of representation of real-world fuel consumption, as confirmed by their verification,
- the proposed estimation method allows fuel consumption to be determined without interfering with the design of the engine systems,
- future research should verify the models for different external conditions through in-flight engine tests.

Acknowledgements

The presented results have been cofinanced from the subsidies appropriated by the Ministry of Science and Higher Education – 0416/SBAD/0004.

Nomenclature

s_i	instantaneous signal value	RMS	Root Mean Square value of signal
N	number of signal samples analysed	PEAK	peak value of signal
FC	fuel consumption		

Bibliography

[1] Adams M. Rotating machinery vibration: from analysis to troubleshooting. 2nd edition, CRC Press, Taylor & Francis Group 2009.
[2] Alili B, Hafaifa A, Iratni A. Faults detection based on fuzzy concepts for vibrations monitoring in gas turbine. Diagnostyka. 2020;21(4):67-77. https://doi.org/10.29354/diag/129581
[3] Alotaibi M, Honarvar Shakibaei Asli B, Khan M. Non-invasive inspections: a review on methods and tools. Sensors. 2021;21:8474. https://doi.org/10.3390/s21248474
[4] Avramchuk VS, Kazmin VP. Estimation of combustion engine rotation speed based on vibration signal analysis. KEM. 2016;685:436-440. https://doi.org/10.4028/www.scientific.net/kem.685.436
[5] Baker R. Flow Measurement Handbook. Industrial designs, operating principles, performance, and applications. 2nd Edition, Cambridge University Press 2016.
[6] Balicki W. The needs and methods of diagnostics of aeronautical turbine engines. Proceedings of the Institute of Aviation. No. 199. Scientific publications of the Institute of Aeronautics 2009.
[7] Boguś P, Cieszyński M, Merkisz J. Multiresolution analysis of vibration signals acquired from locomotive Diesel engine for classification of engine states basing on signal statistical parameters. Combustion Engines. 2017;168(1):68-72. https://doi.org/10.19206/CE2017-111
[8] Bouaouiche K, Menasria Y, Khalifa D. Detection of defects in a bearing by analysis of vibration signals, Diagnostyka. 2023;24(2):1-7. https://doi.org/10.29354/diag/162230
[9] Cempel C, Haddad SD. Vibroacoustic Condition Monitoring, Ellis Horwood, New York 1991 (translate from polish) Bookmark.
[10] Chachurski R, Balicki W, Głowacki P. Aircraft power units. Part 3: Diagnostics. Military Academy of Technology 2016.
[11] Crabtree M. The Concise Industrial Flow Measurement Handbook. A definitive practical guide. CRC Press, Taylor & Francis Group 2020.
[12] Czechyra B, Szymański GM, Tomaszewski F. Assessment of cam valves clearance in internal combustion engine based on parameters of vibration – methodological assumption. Combustion Engines. 2004;118(1):51-59. https://doi.org/10.19206/CE-117424
[13] Fabiś P, Flekiewicz B, Flekiewicz M. On board recognition of different fuels in SI engines with the use of dimensional and non-dimensional vibration signal parameters. Combustion Engines. 2009;136(1):69-75. https://doi.org/10.19206/CE-117222
[14] Fabry S, Ceskovic M. Aircraft gas turbine engine vibration diagnostic. Czech Technical University in Prague. Magazine of Aviation Development. 2017;5(4):24-28.
[15] Grajek L, Kałuszka M. Statistical conclusion – models and methods. Scientific-Technical Publishing House, Warsaw 2000.
[16] Gubran AA, Sinha JK. Shaft instantaneous angular speed for blade vibration in rotating machine. Mech Syst Signal Pr. 2014;44(1-2):47-59. https://doi.org/10.1016/j.ymssp.2013.02.005
[17] Jałowiecki A, Fidali M, Krol A. Investigation of rolling bearing lubrication condition. Diagnostyka. 2021;22(4):51-58. https://doi.org/10.29354/diag/144123
[18] LaNasa P, Loy Upp E. Fluid flow measurement, a practical guide to accurate flow measurement. 3rd edition. Butterworth-Heinmann 2014.
[19] Łączkowski R. Vibroacoustics of machinery and equipment. Wydawnictwa Naukowo-Techniczne, Warsaw 1983.
[20] Marsili R, Tomassini R, Rossi G. A calibration technique for non contact measurement systems of jet engine blades vibration during operation. 2017 IEEE International Workshop on Metrology for AeroSpace (MetroAeroSpace). Padua, Italy 2017;489-495. https://doi.org/10.1109/MetroAeroSpace.2017.7999624
[21] Merkisz J, Waligórski M. Recognition of combustion process irregularities in small volume displacement diesel engines with the use of non-dimensional characteristics of the

vibration signal. Combustion Engines. 2017;169(2):18-23. https://doi.org/10.19206/CE-2017-204
[22] Muszynska A. Vibrational diagnostics of rotating machinery malfunctions. International Journal of Rotating Machinery. 1995;1(3-4):237-266. https://doi.org/10.1155/S1023621X95000108
[23] Ogundare J. Understanding least Squares estimation and geomatics data analysis. Wiley 2019.
[24] Peeters C, Leclerc Q, Antoni J, Guillaume P, Helsen J. Vibration-based angular speed estimation for multi-stage wind turbine gearboxes. IOP Conf. Series: Journal of Physics: 2017;842:012053. https://doi.org/10.1088/1742-6596/842/1/012053
[25] Piezoelectric charge accelerometer types 4391 and 4391-V. 2022. https://www.bksv.com/-/media/literature/Product-Data/bp2039.ashx
[26] Randall R. Vibration-Based Condition Monitoring: Industrial, Aerospace and Automotive Applications. Wiley 2011.
[27] Serridge M, Licht TR. Piezoelectric accelerometers and vibration preamplifiers. Brüel & Kjær 1987.
[28] Spitzer D. Industrial flow measurement. 3rd ed. The Instrumentation, Systems, and Automation Society 2005.
[29] Sujatha C. Vibration, Acoustics and Strain Measurement, Theory and Experiments. Springer 2023. https://doi.org/10.1007/978-3-031-03968-3
[30] Szymański GM, Misztal W. Analysis of measurement points sensitivity of vibration signals on the stand of jet engine. Combustion Engines. 2017;171(4):279-282. https://doi.org/10.19206/CE-2017-448
[31] Szymański GM, Tomaszewski F. Diagnostic aspects of natural frequencies of selected elements of internal combustion engines. Logistics 2010.
[32] Zimroz R, Urbanek J, Barszcz T, Bartelmus W, Millioz F et al. Measurement of instantaneous shaft speed by advanced vibration signal processing – application to wind turbine gearbox. Metrology and Measurement Systems. 2011;4:701-712. https://hal.science/hal-00661222
[33] Sujatha C. Vibration and Acoustics: Measurement and Signal Analysis. 1st ed. New York, McGraw-Hill Education 2010.

Prof. Grzegorz M. Szymański, DSc., DEng. – Institute of Transport, Poznan University of Technology, Poland.
e-mail: *grzegorz.m.szymanski@put.poznan.pl*

Bartłomiej Cywka, Lt, MEng. – 31st Tactical Air Base, Poznan-Krzesiny, Poland.
e-mail: *bartlomiej.cywka@gmail.com*

Daniel Mokrzan, MEng. – Institute of Transport, Poznan University of Technology, Poland.
e-mail: *daniel.mokrzan@put.poznan.pl*

Wojciech Prokopowicz, Col. DEng. – Inspectorate of Armed Forces Support, Bydgoszcz, Poland.
e-mail: *wojciech.prokopowicz@put.poznan.pl*